Funded by the Horizon 2020 Framework Programme of the European Union

Grant Agreement nr.: 687008

Project acronym: GOTSolar

Project full title: New technological advances for the third generation of solar cells

Deliverable D3.5 – Identification of promising HTMs with strong light absorption in the visible to NIR region exceeding 900 nm to use as dual absorbers (Public)

Start date of the project: 01/01/2016	**Project coordinator name**: Adélio Mendes
Duration of the project: 36 months	**Institution of the Project coordinator:** UPORTO
	WP Reference: WP3
Period covered by this report: from 1/1/2016 to 30/04/2018	**WP leader name:** Peter Bäuerle
Nr. pages: 12	**Institution of the WP leader:** UULM

Funded by the Horizon 2020 Framework Programme of the European Union

GOT SOLAR

Contents

Funded by the Horizon 2020 Framework Programme of the European Union

1. Introduction

In the reporting period, a series of novel small band-gap hole transport materials (HTMs) were successfully synthesized and characterized. The structures are based on heteroacene core units and were tailored for application in perovskite solar cells (PSC). The small band gap molecules **UU2-UU6** were designed in a donor (D)-π-bridge-acceptor (A) (D-π-A) fashion. The combination of an electron-rich D and electron-deficient A moiety in the conjugated backbone of a molecule leads to a lowering of the HOMO-LUMO energy gap and to a strong bathochromic and hyperchromic shift of the absorption. The effect can be further enhanced by elongating the π-bridge. Thus, in the case of derivatives **UU2-UU6**, the π-bridge is composed of a series fused rings, forming planar and rigid cores.. As donor moiety, a triphenyl-amine (TPA) was attached at one end of the heteroacene π-bridge in order to raise the HOMO energy level. At the other end two different acceptor groups with different acceptor strength were attached in order to lower the LUMO energy level. This series of small band gap HTMs were investigated by UV-Vis spectroscopy and cyclic voltammetry in order to determine the optical and electronic properties (Table 1).

2. Synthesis

The synthesis for all HTMs starts with the corresponding core which is always mono-formylated in one of the two thiophene α-positions to enable the introduction of acceptor groups by Knoevenagel condensation. As a second step, the remaining free thiophene α-position is brominated to open the molecule for the implementation of the triarylamine donor moiety. As a last step one of the two possible acceptor groups is introduced by Knoevenagel condensation to finish the D-π-A HTM.

The synthesis of the two HTMs **UU2** and **UU3** starts with the core The first step is a mono-formylation utilizing the Vilsmeier-Haack reaction with phosphoryl chloride and dimethyl formamide in 80% yield. The remaining free thiophene α-position is brominated with *N*-bromosuccinimide, followed by a cross coupling to introduce the triarylamine substituent. A Knoevenagel condensation is used in the last step to form **UU2** and **UU3**, respectively.

The HTMs **UU4** and **UU5** were synthesized analogous to **UU2** and **UU3** but the synthesis starts with a different core. The yields were comparable to those of **UU2** with a slightly lower yield for the cross-coupling.

The synthesis of the HTM **UU6** starts with the last core. The yields for each synthetic step are slightly decreased comparing other derivatives. Only on derivative has been synthesized in this series. The derivative with the stronger acceptor group has not been and won't be synthesized due to expected problems with the frontier molecular orbital (FMO) levels. The

LUMO value of the derivative would most probably be too high to be applicable in PSCs. Details can be found on page 11.

3. Optical and electrochemical characterization

All HTMs were characterized utilizing UV-Vis absorption spectroscopy and cyclic voltammetry. The absorption spectra of HTMs **UU2**, **UU4**, and **UU6** are shown in Figure 1. All spectra were measured in dichloromethane (DCM) at room temperature. For the HTM **UU2** we can observe three different absorption bands at 307, 392 and 591 nm. The most red-shifted absorption band with a maximum at 591 nm exhibits an extinction coefficient of 93 700 $M^{-1}cm^{-1}$. The absorption onset is at 667 nm corresponding to an optical gap of 1.86 eV. The HTM **UU4** shows also three absorption bands at 307, 402, and 594 nm. The absorption maximum at 594 nm has an extinction coefficient of 94 300 $M^{-1}cm^{-1}$. The absorption onset is at 674 nm which leads to an optical gap of 1.84 eV. The last HTM **UU6** shows absorption bands at 309, 411, and 615 nm. The maximum at 615 nm exhibits an extinction coefficient of 75 900 $M^{-1}cm^{-1}$. The material has an absorption onset of 697 nm corresponding to an optical gap of 1.78 eV. By comparing the optical properties through the series several trends are visible. The low energy band exhibits a red shift of 3 nm from **UU2** to **UU4** and a large 21 nm red shift from **UU4** to **UU6**. The same is the case for the absorption band at around 400 nm. From **UU2** to **UU4** we observe a red shift of 10 nm, from **UU4** to **UU6** of another 9 nm. **UU6** shows a hypochromic shift of the low energy absorption band compared to **UU4** and **UU2** which practically have the same extinction coefficients. The absorption band at around 400 nm shows a hyperchromic shift from **UU2** to **UU4** and **UU6**. This absorption band is assigned to the corresponding cores which explaines the hyper- and bathochromicity happening due to elongation of the π-system.

Funded by the Horizon 2020 Framework Programme of the European Union

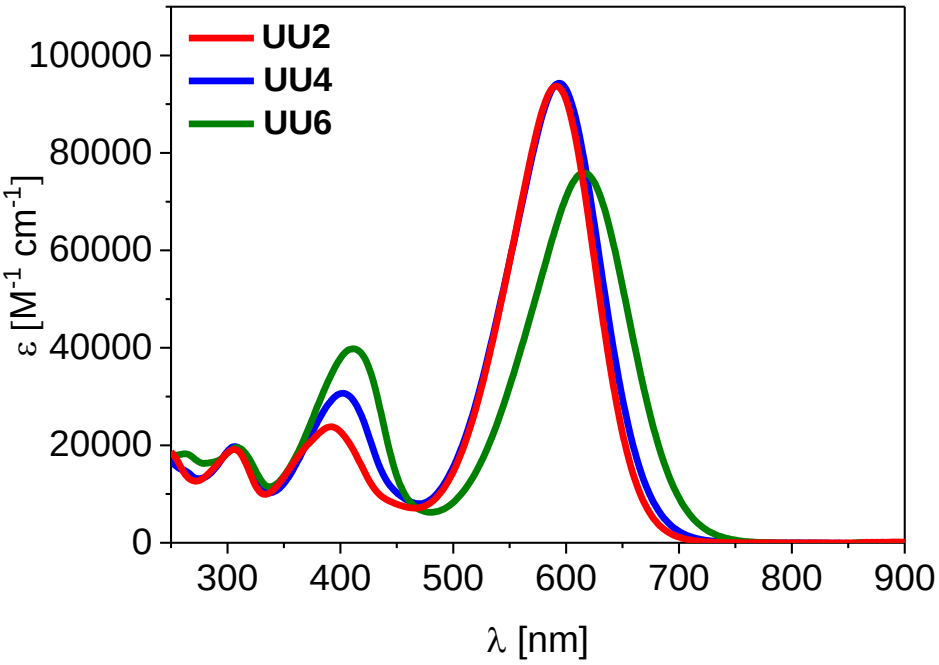

Figure 1: Solution UV-Vis absorption spectra of HTMs UU2, UU4, and UU6, measured in DCM.

The absorption spectra of HTMs **UU3** and **UU5** are shown in Figure 2. The spectra were measured in DCM at room temperature. Both spectra show three different absorption bands. The lowest energy band has a maximum at 732 nm for **UU3** and **UU5**. The extinction coefficients are comparable with 116 700 $M^{-1}cm^{-1}$ for **UU3** and 111 400 $M^{-1}cm^{-1}$ for **UU5**. The absorption onset lies at 843 nm for **UU3** and at 849 nm for **UU5**. The corresponding optical gaps are 1.47 eV for **UU3** and 1.46 eV for **UU5**. The HTM **UU3** shows two more absorption bands, one at 394 nm and one at 309 nm. The band at 394 nm corresponds to the backbone and is also present at the other HTM **UU2**. The last absorption band at 309 nm, which is also present in the spectrum of **UU5**, corresponds to the arylamine. For the HTM **UU5** the absorption band of the backbone lies at 403 nm comparable to the corresponding absorption band at 402 nm for **UU4**.

Funded by the Horizon 2020 Framework Programme of the European Union

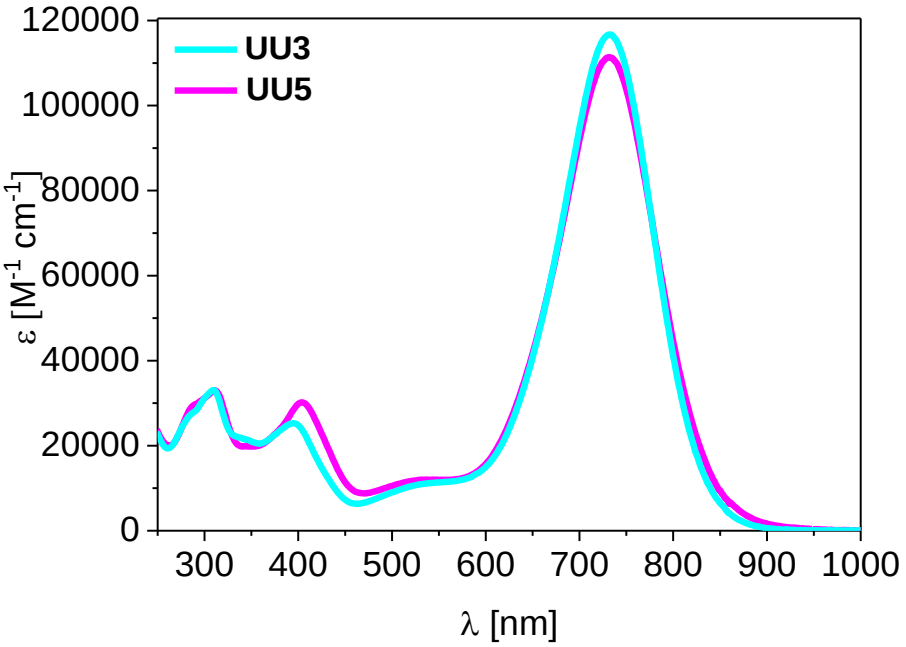

Figure 2: Solution UV-Vis absorption spectra of HTMs UU3 and UU5, measured in DCM.

A comparison between the absorption spectra of **UU2** in Figure 1 and **UU3** in Figure 2 shows the influence of the stronger acceptor group. The main absorption band exhibits a bathochromic shift of 141 nm and the extinction coefficient increases by 23 000 M^{-1} cm^{-1}. The same effect is visible for **UU5** compared to **UU3**.

The cyclic voltammograms of the HTMs **UU2**, **UU4**, and **UU6** are shown in Figure 3. All voltammograms were measured in dry DCM with tetrabutylammonium hexafluorophosphate as supporting electrolyte. A scan rate of 100 mV/s was used. All potentials are internally referenced against the ferrocene/ferrocenium redox pair. The oxidation and reduction potentials were determined for all materials. The ferrocene HOMO energy level was taken to be -5.1 eV vs. vacuum. All HTM FMO levels were determined by the onset of the oxidation and reduction. The electrochemical gap was determined to be the difference between HOMO and LUMO. We can observe two reversible oxidation waves and one irreversible reduction wave for each HTM. The first oxidation of **UU2** occurs at 0.06 V, the second at 0.30 V. For the HTM **UU4** the first oxidation is slightly shifted to lower potentials due to elongation of the π-system and occurs at 0.04 V. The second oxidation is at 0.30 V and is therefore not shifted. The effect of the extended conjugation is again visible for the **UU6** with oxidations at -0.01 V and 0.26 V. The size of the π-system also has a slight influence on the reduction potential. The reduction occurs at -1.76 V for **UU2**, at -1.66 for **UU4** and at -1.62 for **UU6**. This shows that elongation of the core leads to more positive reduction potentials. The HOMO energy level for **UU2** was calculated to be -5.10 eV. For the materials **UU4** and **UU6** a slightly elevated HOMO, which is located at -5.08 eV and -5.06 eV respectively, was obtained. The LUMO energy level experiences the opposite effect starting at -3.53 eV for **UU2** and being lowered to -3.57 eV for **UU4** and -3.62 eV for **UU6**. This leads to electrochemical gaps of 1.57 eV for **UU2**, 1.51 eV for **UU4** and 1.44 eV for **UU6**.

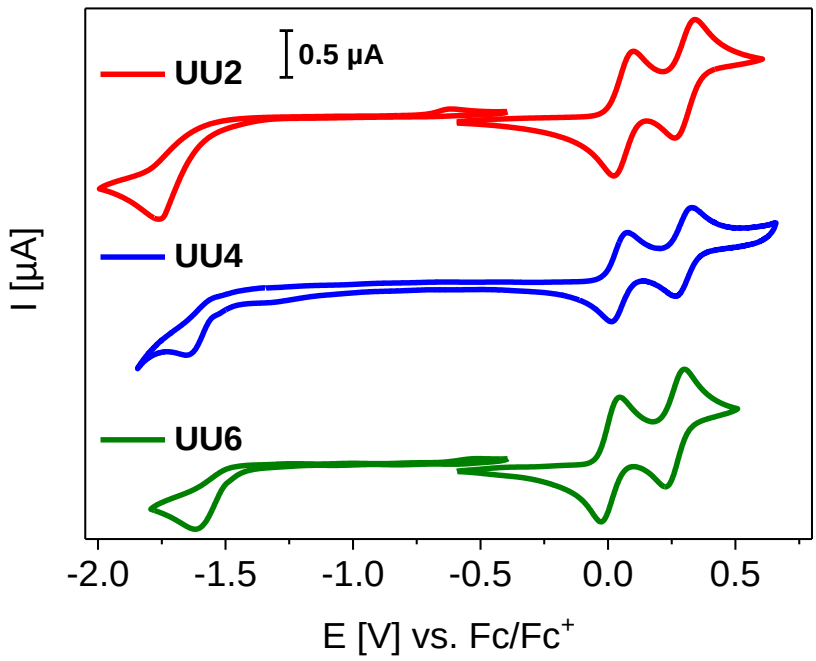

Figure 3: Cyclic voltammograms of HTMs UU2, UU4, and UU6.

Cyclic voltammograms of the HTMs **UU3** and **UU5** were also measured. The above conditions have also been used here. Only for **UU3** dichloroethane had to be used at 65 °C due to the lower solubility. The cyclic voltammograms are shown in Figure 4. Both materials show two oxidation and one reduction wave. For **UU3** we observe the first oxidation at -0.02 V and the second at 0.25 V. For **UU5** the first oxidation occurs at 0.07 V and the second at 0.36 V. This shift to more positive potentials compared to **UU3** is counter intuitive because a shift to more negative potentials is expected by elongation of the π-system. The discrepancy can probably be attributed to the change of solvent and the elevated temperature.[1] The reduction potentials for the derivatives **UU3** and **UU5** are shifted by around 460 and 330 mV respectively. Compared to the corresponding HTMs **UU2** and **UU4**. This strong shift is again attributed to the greater acceptor strength. A HOMO energy level of -4.99 eV was obtained for **UU3**. Compared to **UU2** the HOMO energy level is elevated by 0.11 eV. The HTM **UU5** shows a HOMO of -5.08 eV. For **UU3** a LUMO energy level of -3.87 eV and for UU5 of -3.93 eV was obtained. The elevation of the LUMO energy level, compared to the corresponding materials **UU2** and **UU4**, is 34 and 36 meV respectively. For **UU3** an electrochemical gap of 1.12 eV was obtained. Compared to HTM **UU2** a narrowing of the gap by 0.45 eV takes place. The material **UU5** shows an electrochemical gap of 1.15 eV. The enlargement of the gap from **UU3** to **UU5** is probably again caused by the different measurement method. From the structure and the UV-Vis measurement of **UU5** we would expect a smaller or similar gap than **UU3**.

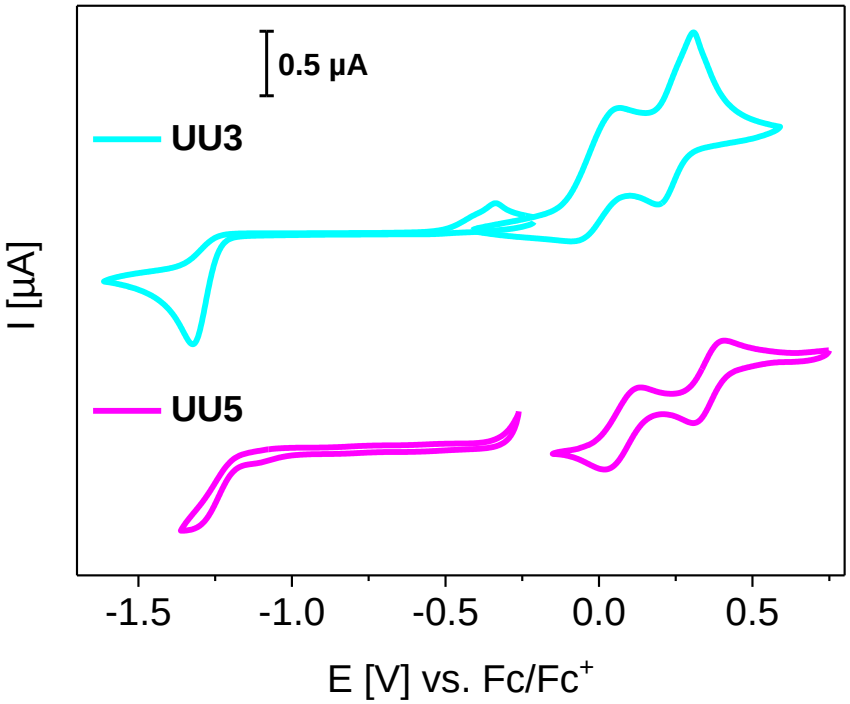

Figure 4: Cyclic voltammograms of HTMs UU3 and UU5.

The summarized optoelectronic properties of HTMs **UU2-UU6** are shown in Table 1.

Table 1: Optoelectronic properties of HTMs UU2-UU6.

	λ_{max} [nm] [a]	ε [M^{-1} cm^{-1}]	E_g^{opt} [eV][b]	E_{ox1} [V]	E_{ox2} [V]	E_{red} [V]	HOMO [eV][c]	LUMO [eV][c]	E_g^{CV} [eV]
UU2	591	93 700	1.86	0.06	0.30	-1.76	-5.10	-3.53	1.57
UU4	594	94 300	1.84	0.04	0.30	-1.66	-5.08	-3.57	1.51
UU6	615	75 900	1.78	0.01	0.26	-1.62	-5.06	-3.62	1.44
UU3	732	116 700	1.47	-0.02	0.25	-1.31	-4.99[c]	-3.87[c]	1.12[c]
UU5	732	111 400	1.46[d]	0.07[d]	0.36[d]	-1.33[d]	-5.08[c,d]	-3.93[c,d]	1.15[c,d]

[a] Measured in dichloromethane. [b] Determined by $E_g = hc/\lambda_{onset}$. [c] Calculated from the onset values of the corresponding redox waves; Fc/Fc^+ was set to -5.1 eV vs. vacuum. [d] Measured in dichloroethane at 65 °C.

The determination of the optoelectronic properties showed that the HOMO energy levels of all D-π-A derivatives **UU2-UU6** lie between -5.10 and -4.99 eV. Therefore the materials seem to be appropriate for their use as HTM in perovskite solar cells. Furthermore, they exhibit very strong absorptions in the visible range of the solar spectrum (λ_{max}=590-730 nm, ε=75,900-110,000 M^{-1} cm^{-1}) depending on the length of the conjugated heteroacene backbone and the strength of the implemented acceptor. The optical gaps of the HTMs were below 1.9 eV for the materials **UU2**, **UU4**, and **UU6.** The last materials UU3 and UU5 show optical gaps below 1.5 eV. Thus, the data clearly show that elongation of the π-bridge on one

hand and increasing strength of the acceptor leads to a bathochromic shift of the absorption, an increased extinction coefficient, reduced redox potentials, lowered HOMO and elevated LUMO energy values, and reduced gaps.

The discrepancy in the obtained values from optical and electrochemical characterization needs to be addressed. The optical characterization in solution usually leads to larger gaps as the gaps obtained through electrochemical characterization. UV-Vis characterization of a thin film would lead to underestimation of the gap because the measured energy of the onset wavelength would only be enough to create an exciton. Therefore the optical gap doesn't consider the energy which is needed for the charge separation of the bound electron-hole pair. The electrochemical gap gives a better approximation and factors in the electron-hole binding energy.[2] The experimentally obtained electrochemical gaps can be converted to new absorption thresholds where charge separation occurs for each material. For the materials **UU2**, **UU4**, and **UU6** we obtain wavelengths of 790, 821 and 861 nm. For derivatives **UU3** and **UU5** we obtain values of 1107 and 1078 nm.

The FMO levels of all synthesized HTMs as well as the conduction bands of titanium dioxide (TiO_2), indium tin oxide (ITO), the valence band of gold (Au), the conduction and valence band of the mixed cation Perovskite $(FAPbI_3)_{0.85}(MAPbBr_3)_{0.15}$ (P) are shown in Figure 5. In perovskite solar cells (PSC) the light absorption and following excitation takes place at the perovskite. The electron is then injected into the conduction band of the electron transport material TiO_2. The hole in the valence band of the Perovskite is injected into the HTM and from the HTM to the gold electrode. Charge transport problems in the solar cell can arise if the energy levels of all involved materials are not adapted.

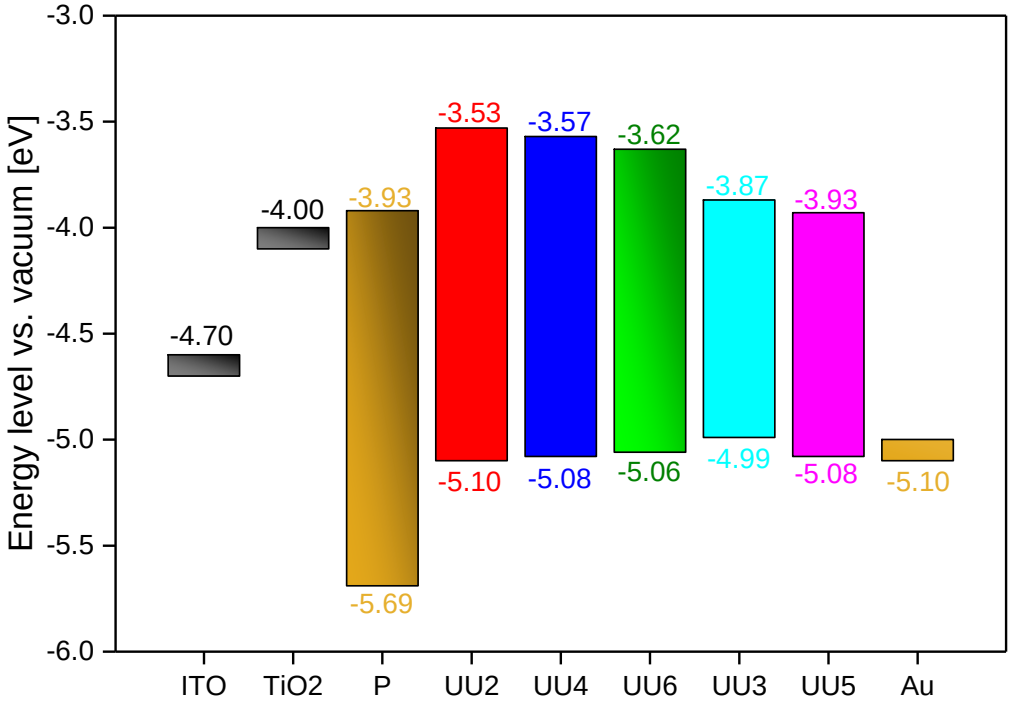

Figure 5: Energy level diagram of compounds and materials utilized in perovskite solar cells.

A closer look at Figure 5 shows possible occurring problems with the synthesized materials. All measured HOMO energy levels, with the exception of **UU2**, are above the conduction band of gold. This should make the injection of a hole from the HTM to the electrode difficult. But previously obtained results indicate that HTMs with HOMO energy levels of -5.0 eV are still applicable. [3-4] For the HTMs **UU3** and **UU5** another problem could arise because of the deep lying LUMO energy level. **UU5** shows a LUMO energy level which is aligned to the conduction band of the perovskite. This could lead to a competing mechanism where the electron from the excited perovskite is not injected into the conduction band of the TiO_2 but into the LUMO (more precisely the conduction band) of the HTM. This process could lead to a loss of efficiency for the solar cell. If the HTM is also to be used as absorber material in the solar cell, it should have a LUMO energy level below the conduction band of the electron transport material. For HTMs **UU2**, **UU4**, and **UU6** this is the case. The FMO energy levels for **UU3** and **UU5** begin to advance into the critical region were problems arise with all the discussed charge transport processes. The material with the smallest optical gap **UU5** is seen as a threshold were the beneficial aspects of a lowered energy gap would be compensated by the lowered efficiency of the charge transport due to misaligned FMO energy levels. Further elongation of the π-system would lead to a worsening of the situation and therefore the last HTM of the series the has not been and won't been synthesized.

Funded by the Horizon 2020 Framework Programme of the European Union

References

[1] N. G. Tsierkezos, *J. Solution Chem.* **2007**, *36*, 289-302.
[2] J.-L. Bredas, *Mater. Horiz.* **2014**, *1*, 17-19.
[3] L. Calió, S. Kazim, M. Grätzel, S. Ahmad, *Angew. Chem. Int. Ed.* **2016**, *55*, 14522-14545.
[4] L. Calió, S. Kazim, M. Grätzel, S. Ahmad, *Angew. Chem.* **2016**, *128*, 14740-14764.